Available online at www.sciencedirect.com
ScienceDirect
Chinese Journal of Natural Medicines 2019, **17**(8): 0608–0615
Chinese Journal of Natural Medicines

Investigation into perturbed nucleoside metabolism and cell cycle for elucidating the cytotoxicity effect of resveratrol on human lung adenocarcinoma epithelial cells

LI Zheng[1], CHEN Qian-Qian[1], LAM Christopher Wai Kei[2], GUO Jian-Ru[1], ZHANG Wei-Jia[3], WANG Cai-Yun[1], WONG Vincent Kam Wai[1], YAO Mei-Cun[3*], ZHANG Wei[1*]

[1] *State Key Laboratory of Quality Research in Chinese Medicines and Macau Institute for Applied Research in Medicine and Health, Macau University of Science and Technology, Macau 999078, China;*
[2] *Faculty of Medicine, Macau Institute for Applied Research in Medicine and Health, Macau University of Science and Technology, Macau 999078, China;*
[3] *School of Pharmaceutical Sciences, Sun Yat-sen University, Guangzhou 510006, China*

Available online 20 Aug., 2019

[ABSTRACT] In an effort to understand the molecular events contributing to the cytotoxicity activity of resveratrol (RSV), we investigated its effects on human lung adenocarcinoma epithelial cell line A549 at different concentrations. Cellular nucleoside metabolic profiling was determined by an established liquid chromatography-mass spectrometry method in A549 cells. RSV resulted in significant decreases and imbalances of deoxyribonucleoside triphosphates (dNTPs) pools suppressing subsequent DNA synthesis. Meanwhile, RSV at high concentration caused significant cell cycle arrest at S phase, in which cells required the highest dNTPs supply than other phases for DNA replication. The inhibition of DNA synthesis thus blocked subsequent progression through S phase in A549 cells, which may partly contribute to the cytotoxicity effect of RSV. However, hydroxyurea (HU), an inhibitor of RNR activity, caused similar dNTPs perturbation but no S phase arrest, finally no cytotoxicity effect. Therefore, we believed that the dual effect of high concentration RSV, including S phase arrest and DNA synthesis inhibition, was required for its cytotoxicity effect on A549 cells. In summary, our results provided important clues to the molecular basis for the anticancer effect of RSV on epithelial cells.

[KEY WORDS] Resveratrol; LC-MS; Deoxyribonucleotides; DNA synthesis; S phase arrest

[CLC Number] R965, R969.1 **[Document code]** A **[Article ID]** 2095-6975(2019)08-0608-08

Introduction

Resveratrol (3, 4', 5-trihydroxy-trans-stilbene, RSV) is a phytoalexin, which was first isolated from the roots of white hellebore in 1940 [1]. Since then, RSV has been found in a wide range of plant species, a number of which are components of the human diet, including mulberries, peanuts and grapes. RSV is a kind of typical polyphenolic phytoalexin that is produced in response to exogenous stress factors [2]. This molecule has been the focus of a number of studies investigating its beneficial effects on neurological, hepatic, and cardiovascular systems, including cardiovascular protective [3], antiplatelet [4], antioxidant [5], antiinflammatory [6], and blood glucose-regulating effects [7-9]. In recent years, interest in RSV has focused on its anti-cancer activity. RSV is closely related to the growth inhibition in various cancer cells, including stomach, prostate, lung, myeloid, breast, liver, pancreas, prostate, skin, and colon [10-13]. However, the anti-cancer mechanism of RSV has not yet been univocally elucidated. There is a common view that RSV can affect cell conditions by modulating the activities of various intercellular enzymes including (but not limited to) ribonucleotide reductases (RNR), lipo- and cyclooxygenases, DNA polymerases and other proteins [14-16], of which RNR inhibition effect was broadly reported in recent years.

RNR is a fundamental complex enzyme existing in almost all free living organisms, parts of double-stranded DNA

[Received on] 13-May-2019
[Research funding] This work was supported by the Macao Science and Technology Development Fund (FDCT, No. 0052/2018/A2).
[*Corresponding authors] E-mails: Yaomeicun@gmail.com (YAO Mei-Cun); Wzhang@must.edu.mo (ZHANG Wei)
These authors have no conflict of interest to declare.

viruses and some bacteria. RNR can catalyze the reduction of ribonucleosidediphosphates into corresponding deoxyribonucleoside diphosphates (dNDPs) which is a rate-limiting step for deoxyribonucleoside triphosphates (dNTPs) synthesis [17]. Human RNR is composed of three known subunits, RRM1 (large subunit), RRM2 (small subunit) and an encoded P53-controlled ribonucleotide reductase (P53R2) that are differentially regulated during the cell cycle [18]. Interestingly, the level of the relative large part RRM1 is more constant throughout the cell cycle, while the small unit RRM2 showing a distinct change in express level which indicates that RRM2 might donate more in regulating RNR's activity. Fontecave *et al*. suggested that a stoichiometric amount of RSV can destroy the tyrosyl radical in protein R2 causing inhibition of RNR activity [14, 17-19]. However, the subsequent effects, such as disturbing dNTPs supply for DNA replication, were not further investigated.

Ribonucleotides (RNs) and deoxyribonucleotides (dRNs) play an important role in a broad range of key cell functions. Unbalanced cellular pools of dNTPs, dNDPs and deoxyribonucleoside monophosphates (dNMPs) are suggested mutagenic. Thus, the perturbation of cellular RNs and dRNs after RSV treatment can in reverse illustrate the effect of RSV on cell function. Moreover, the changes in cell cycle regulatory processes and perturbation of nucleotide metabolism contributing to the cytotoxicity effect of RSV on A549 cells has not been deeply investigated.

In this study, the effects of RSV on cellular RNs and dRNs pools were investigated by an established liquid chromatography-mass spectrometry (LC-MS) method [20]. Cell cycle analysis and western blot analysis were performed to investigate RSV mechanisms of anti-proliferation and perturbating cellular nucleotide metabolism. Hydroxyurea (HU), an inhibitor of RNR activity which is the only ribonucleotide reductase tyrosyl radical scavengers used clincally [14], was used as a reference. We found that investigation of cellular nucleotide metabolism is an effective approach to facilitate our understanding of the anti-tumor mechanism of RSV.

Materials and Methods

Chemicals and reagents

Resveratrol (purity 99%) was purchased from Zheng-Zhou HuaWen Chemical Co., Ltd. (HeNan, China). Human lung adenocarcinoma epithelial cell line A549 was supplied by American Type Culture Collection (ATCC, Rockville, MD, USA). Phosphate buffer saline (PBS), RPMI medium 1640, 0.25% Trypsin-EDTA solution, penicillin-streptomycin solution, and fetal bovine serum (FBS) were obtained from GIBCO Invitrogen Co. (Carlsbad, CA, USA). A Cell Cycle Analysis Kit was purchased from Signal-way Antibody Co., Ltd. (College Park, MD, USA). Trichloroacetic acid (TCA), hexylamine (HA), diethylamine (DEA), trioctylamine, 1, 1, 2-trichlorotrifluoroethane and stable isotope labeled adenosine-$^{13}C_{10}{}^{15}N_5$-triphosphate ($ATP^{13}C^{15}N$) were purchased from Sigma-Aldrich Chemical Co. (St. Louis, MO, USA). LC-MS grade methanol, acetonitrile, dimethyl sulfoxide (DMSO) and acetic acid were purchased from Anaqua Chemical Supply Co. (Houston, TX, USA). Ultra-pure water was obtained from the Milli-Q Gradient Water System (Millipore Corporation, Billerica, MA, USA).

Cell Culture

A549 cells were cultured in RPMI Medium 1640 supplemented with 10% FBS, 100 UI·mL^{-1} penicillin, and 100 μg·mL^{-1} streptomycin in humidified air at 37 °C with 5% CO_2.

Cell viability assay

The cytotoxic effect of RSV and HU on A549 cells was determined by the MTT (Sigma-Aldrich Chemical Co., St. Louis, MO, USA) assay. A549 cells were seeded in 96-well plates (LabServ, Thermo Fisher Scientific Co., Beijing, China) at density of 1.5×10^4 cells/well. After 24 h incubation, cells were treated with RSV and HU at different concentrations (12.5, 25, 50, 100, 200 μmol·L^{-1} RSV and 1 mmol·L^{-1} HU) for further 24 h. MTT solution (final concentration of 0.5 mg·mL^{-1} in medium) was added to each well and incubated further for 4 h. Then the supernatant medium was removed, and 100 μL of DMSO was added to each well to dissolve the purple crystals of formazan. Absorbance was measured with a microplate reader (Infinite M200 PRO, Tecan Austria GmbH 5082, Grödig, Austria) at 570 nm, *vs* 650 nm as the reference wavelength.

Preparation of cell pellets

A549 cells were seeded in 100 mm × 20 mm dishes (LabServ, Thermo Fisher Scientific, Beijing, China). After overnight culture, cells of the treatment group were incubated with 25 or 100 μmol·L^{-1} RSV and 1 mmol·L^{-1} HU for 24 h, respectively. Control cells were incubated in medium only. At the end of the incubation, cells of each group were washed with ice-cold PBS twice and trypsinized with 0.25% trypsin-EDTA. Cells from control groups and treatment groups were then re-suspended in 10 mL ice-cold PBS and centrifuged for 5 min at 1500 r·min^{-1}. The cell pellets were incubated with 150 μL of 15% TCA containing 7.5 μL of 20.0 μmol·L^{-1} $ATP^{13}C$, ^{15}N as internal standard and put on ice for 5 min for protein precipitation. After centrifugation at 13 500 r·min^{-1} for 15 min at 4 °C, the acidic supernatant was separated and neutralized twice with 100 μL mixture of 1, 1, 2-trichlorotrifluoroethane and trioctylamine (a volume ratio of 55 to 45). Samples were stored at –80 °C until analysis within two days.

Detection of cellular RNs and dRNs pools by LC-MS/MS

The proofing unit comprised a Thermo Fisher TSQ LC-MS/MS system incorporating an Accela pump, an Accela autosampler, and a Quantum Access triple quadrupole mass spectrometer (Thermo Fisher Scientific Co., San Jose, CA, USA). The Xcalibur software version 2.0.7 (Thermo Fisher Scientific Co., San Jose, CA, USA) and the Thermo LCquan 2.5.6 (Thermo Fisher Scientific Co., San Jose, CA, USA) data analysis program were used for the data acquisition and data

processing, respectively. The chromatographic separation was performed on an XTerra® MS C_{18} column (3.5 μm, 2.1 mm × 150 mm, Waters Co., Milford, MA, USA). There were two mobile phases using in the analytic system, one was 0.5% DEA-5 mmol·L^{-1} HA in water, pH adjusted to 10 with acetic acid (A), the other was 50% (*V*/*V*) acetonitrile in water (B). The eluents consisted of linear gradient of A and B: 0−15 min, 100%−85% A; 15−35 min, 85%−75% A; 35−45 min, 75%−45% A; 45−50 min, 45%−100% A; 50−60 min, 100% A. For all RN and dRN, the following optimized parameters were obtained. The sheath gas pressure reached 40 psi. The ionspray voltage was set at 3000 V for negative mode and 4000 V for positive mode at a temperature of 350 °C and an auxiliary gas pressure of 15 psi. Quantification was performed using multiple reactions monitoring (MRM) as previously published [20].

Cell cycle analysis

A549 cells were seeded at density of 2.0 × 10^5 cells/well in 6-well plates (LabServ, Thermo Fisher Scientific Co., Beijing, China) in duplicate and incubated with 25, 100 μmol·L^{-1} RSV and 1 mmol·L^{-1} HU for 24 h, respectively. Control cells were incubated in medium only. Cells were harvested and fixed in 70% (*V*/*V*) cold ethanol overnight at 4 °C. The fixed cells were collected by centrifugation and re-suspended in PBS and incubated with 5 mg·mL^{-1} PI (propidium iodide, Sigma-Aldrich, St. Louis, MO, USA) and 10 mg·mL^{-1} RNase A (Ribonuclease A from bovine pancreas, Sigma-Aldrich, St.Louis, MO, USA) at room temperature for 30 min in the dark. Then the cells were analyzed on a flow cytometer (Muse™ cell analyzer, Merck Millipore, Darmstadt, Germany). Finally, the percentages of cells in different phases (G_0/G_1, S and G_2/M) were calculated using Modfit software (Verity Software House, USA).

Western Blot analysis

A549 cells were seeded at density of 2.0 × 10^5 cells/well in 6-well plates and incubated with 25 or 100 μmol·L^{-1} RSV and 1 mmol·L^{-1} HU for 24 h, respectively. Cells of control group were incubated in medium only. All groups of cells were harvested and lysed in RIPA buffer (Cell Signaling Technologies Inc. Beverly, MA, USA). Protein concentration was determined using Bradford reagent (Bio-Rad Laboratories Inc., Hercules, CA, USA). Cell lysates were mixed with 5X SDS-loading buffer (4 : 1, *V*/*V*) and heated at 100 °C with locked capping for 5 min. Samples (40 μg of protein) were resolved on 10% SDS-PAGE and then electroblotted onto polyvinylidene fluoride transfer membrane (Bio Trace™ PVDF, 0.45 μmol·L^{-1}, Pall Life Sciences Co., Mexico) and were incubated with different antibodies including RRM1 (Cell Signaling Technology Inc., MA, USA), RRM2 and p53R2 (Abcam Ltd., Cambridge, UK) and *β*-tubulin (Santa Cruz Biotechnology, CA, USA) overnight at 4 °C, respectively. The membranes were further incubated with HRP-conjugated antibodies for one hour. The protein bands were visualized using the enhanced chemiluminescence reagents (Invitrogen Co., Paisley, Scotland, UK), and were analyzed with the Image J 1.46r software (National Institutes of Health, Bethesda, MD, USA).

Statistical analysis

The data was expressed as mean ± SD values from three independent replicate experiments. *P* value less than 0.05 ($^*P < 0.05$, $^{**}P < 0.01$, compared with control group) was considered to be statistically significant by using Student's *t*-test analysis.

Results and Discussion

Cytotoxicity of RSV and HU on A549 cells

To examine the cellular toxicity effects of RSV and HU, MTT assay was performed with different RSV concentrations in A549 cells. As shown in Fig. 1, 12.5−25 μmol·L^{-1} RSV and 1 mmol·L^{-1} HU did not affect the cell viability after 24 h treatment. The toxicity of RSV was obvious when RSV concentration was more than 50 μmol·L^{-1}. The A549 cell viability decreased in a dose-dependent manner after treatment with RSV at concentrations of 50, 100, 200 μmol·L^{-1}. RSV at concentrations of 100 μmol·L^{-1} significantly inhibited cell viability relative to control cells ($^{**}P < 0.01$) and the cytotoxicity effect of RSV was stronger than HU on A549 cells. In follow-up studies, 25 and 100 μmol·L^{-1} RSV were selected as the low and high concentrations of RSV, respectively.

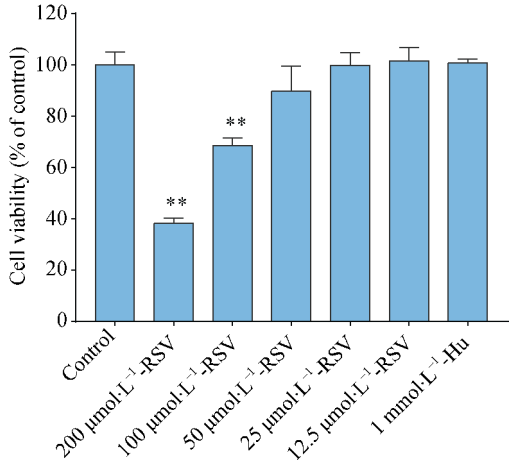

Fig. 1 The effect of RSV and HU on A549 cell viability at different concentrations after 24 h treatment. The data was represented as mean ± SD (n = 6), $^{**}P < 0.01$ *vs* control group

Perturbation of cellular RNs and dRNs pools after RSV and HU treatment

As shown in Table 1, low concentration RSV caused more extensive alterations in RNs pools than high concentration RSV. Significant decreases in ATP and GTP pools, increases in AMP, GDP, GMP and UDP pools were found in A549 cells with 25 μmol·L^{-1} RSV treatment. However, only significant increase in ATP pool occurred in A549 cells treated with 100 μmol·L^{-1} RSV or 1 mmol·L^{-1} HU. In contrast, high concentration RSV resulted in more extensive alterations of dRNs pools than low concentration RSV, which

was similar with the effect of 1 mmol·L^{-1} HU (Table 2). Significant decreases in cellular dATP, dGTP, dTTP, dADP, dCDP, dGDP and dGMP absolute amounts were found in A549 cells after 100 μmol·L^{-1} RSV treatment. Of the four deoxyribonucleoside triphosphates (dNTPs), cellular dGTP pool presented the greatest decrease while cellular dCTP pool showed no significant change, consequently, imbalance of cellular dNTPs occurred after 100 μmol·L^{-1} RSV treatment.

Table 1 RNs pools in A549 cells of different experimental groups (pmol/10^6 cells, mean ± SD, *n* = 3)

	Control	RSV (25 μmol·L^{-1})	RSV (100 μmol·L^{-1})	Hu (1 mmol·L^{-1})
ATP	10 215.06 ± 841.56	9748.71 ± 1987.87*	11 534.48 ± 554.66*	12 104.78 ± 644.8**
ADP	1456.08 ± 405.56	1708.46 ± 223.48	1401.86 ± 493.82	1512.97 ± 347.74
AMP	235.63 ± 101.19	364.33 ± 92.42*	204.01 ± 114.79	209.46 ± 79.2
CTP	973.06 ± 175.45	830.9 ± 145.93	1007.22 ± 92.91	1110.28 ± 143.98
CDP	152.75 ± 32.46	144.5 ± 55.96	121.06 ± 62.62	144.37 ± 36.24
CMP	25.19 ± 7.66	29.95 ± 10.7	23.36 ± 10.47	24.51 ± 13.07
GTP	3033.56 ± 365.99	2108.83 ± 657.36*	2828.75 ± 670.81	3260.64 ± 510.17
GDP	627.73 ± 126.04	861.03 ± 271.99*	602.05 ± 96.84	698.86 ± 84.79
GMP	26.21 ± 10.74	38.18 ± 15.23*	20.38 ± 11.83	21.18 ± 8.71
UTP	6548.61 ± 1415.83	5692.5 ± 1759.93	5311.99 ± 1150.89	7694.93 ± 1555.01
UDP	667.54 ± 196.89	941.58 ± 285.36*	452.4 ± 160.28	640.24 ± 119.36
UMP	34.74 ± 14.87	52.92 ± 15.94	20.88 ± 11.91	25.28 ± 9.06

$^{*}P < 0.05$, $^{**}P < 0.01$ *vs* control group

Table 2 dRNs pools in A549 cells of different experimental groups (pmol/10^6 cells, mean ± SD, *n* = 3)

	Control	RSV (25 μmol·L^{-1})	RSV (100 μmol·L^{-1})	Hu (1 m mol·L^{-1})
dATP	12.53 ± 0.91	10.68 ± 2.5	7.41 ± 1.66**	4.18 ± 1.22**
dADP	1.06 ± 0.29	0.96 ± 0.70	0.31 ± 0.24**	0.13 ± 0.11**
dAMP	0.022 ± 0.001	0.030 ± 0.001	0.031 ± 0.005	0.024 ± 0.003
dCTP	8.49 ± 1.58	11.07 ± 3.83	8.69 ± 2.52	7.10 ± 3.05
dCDP	0.53 ± 0.052	0.80 ± 0.15**	0.28 ± 0.14**	0.37 ± 0.21*
dCMP	0.13 ± 0.01	0.10 ± 0.01	0.13 ± 0.03	0.10 ± 0.02
dGTP	9.42 ± 1.89	6.36 ± 3.86	1.99 ± 1.01**	1.13 ± 0.80**
dGDP	0.51 ± 0.26	0.60 ± 0.073	0.23 ± 0.059*	0.20 ± 0.087*
dGMP	0.42 ± 0.15	0.94 ± 0.32*	0.17 ± 0.11*	0.15 ± 0.06**
dTTP	25.38 ± 4.68	28.59 ± 5.50	20.01 ± 3.58*	14.11 ± 4.61**
dTDP	2.02 ± 0.33	3.61 ± 1.01*	1.75 ± 0.28	1.44 ± 0.20*
dTMP	0.025 ± 0.012	0.044 ± 0.012*	0.019 ± 0.008	0.008 ± 0.005*

$^{*}P < 0.05$, $^{**}P < 0.01$ *vs* control group

In addition, the absolute amount of each RNs and dRNs in A549 cells was used to obtain a data matrix consisting of 24 objects (groups) and 24 variables (RNs and dRNs pools). Supervised orthogonal partial least squares discriminant analysis (OPLS-DA) model was constructed to understand and visualize the complex effect of RSV at different concentrations on RNs and dRNs pools using SIMCA-P version 14.0 (Umetrics Inc., Umeå, Sweden). As shown in Fig. 2A, control groups and treatment groups showed an appreciable separation based on the total alteration in the data. Moreover, 25 μmol·L^{-1} RSV group could be separated from 100 μmol·L^{-1} RSV group, whereas 100 μmol·L^{-1} RSV group and 1 mmol·L^{-1} HU group could not get clear separation.

These results indicated that the perturbation of cellular RNs and dRNs pools induced by RSV was dependent on RSV concentrations. The perturbation range and degree of cellular RNs and dRNs pools was both different between 25 μmol·L^{-1} RSV group and 100 μmol·L^{-1} RSV group. RSV disturbed mainly RNs metabolism at low concentration, while perturbing mainly dRNs metabolism at high concentration. The latter was similar to the effect induced by 1 mmol·L^{-1} HU on A549 cells: 100 μmol·L^{-1} RSV and 1 mmol·L^{-1} HU caused similar perturbation of cellular RNs and dRNs pools in A549 cells, suggesting that they might possess similar mechanism of perturbating nucleotide metabolism.

Cellular dNTPs are essential precursors for DNA synthesis, which is required for replication, recombination and repair, therefore the concentration of dNTPs is strictly controlled.

Perturbations in the absolute and relative concentrations of the four dNTPs may lead to inhibition of DNA replication and activation of the S-phase checkpoint. The activated S-phase checkpoint arrests cell cycle progression and activates DNA repair and at worst, leads to apoptosis [21-22]. In this study, RSV and HU resulted in significant alteration of dNTPs compositions (Fig. 2B). Treatment with RSV and HU resulted in increases in percentages of dCTP and dTTP, correspondingly, decreases in dATP and dGTP proportions in A549 cells. Moreover, the effect of dNTPs imbalance presented a positive correlativity with RSV concentrations. As sufficient levels and relative balance of dNTPs were required for DNA synthesis and DNA replication fidelity, the decreases and imbalance of dNTPs pools induced by RSV at high concentration could inhibit DNA synthesis and consequently, contribute to growth retardation and cell-cycle arrest of A549 cells in this study.

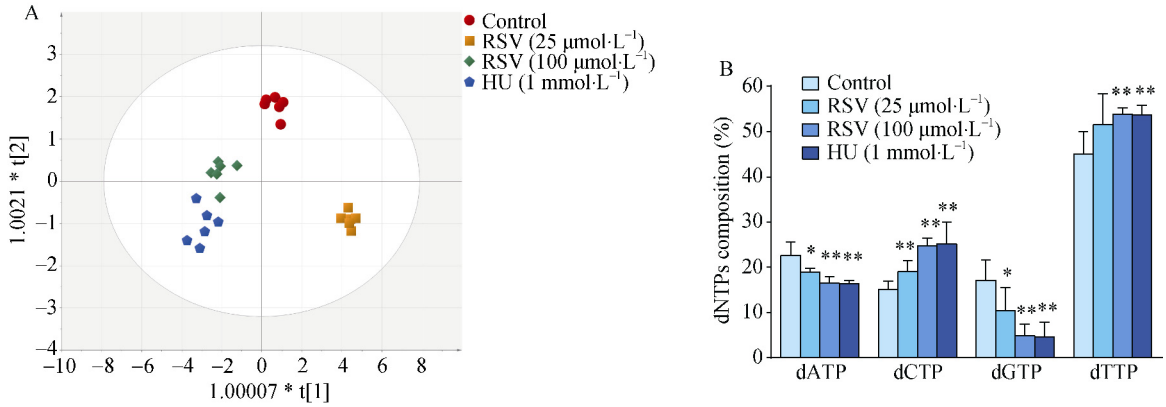

Fig. 2 (A) Imbalance of dNTPs pools in A549 cells induced by RSV and HU. (B) Scores plot of OPLS-DA model for different groups. Scores plot describes the similarities between the *Y*-variables (groups) based on the *X*-variables (RNs and dRNs pools). The data was represented as mean ± SD (n = 3), $^{*}P < 0.05$, $^{**}P < 0.01$ *vs* control group

Cell cycle alteration induced by RSV and HU

Cell proliferation comprises two distinct processes: cell cycle and cell growth. The four phases composing the mammalian cell cycle, including S (DNA synthesis), M (mitosis), G_1 and G_2, are mainly regulated by cyclin-dependent kinases (CDKs), and E3 ubiquitin ligases [23]. Like many cytotoxic agents, RSV affects cell proliferation by disturbing the normal progress of the cell cycle. RSV could interfere with the molecular machinery of the cell cycle which involves various key regulators, such as p21, p27, p53, cyclin D1, cyclin-dependent kinase (CDK) 4 and CDK 6 [24-26]. Furthermore, cell cycle blockage induced by RSV varies according to the cell type, treatment concentration and duration [27]. For example, treatment with 100 μmol·L^{-1} RSV led to G_1 phase cell cycle arrest in human T24 bladder cancer cells [25], whereas induced accumulation of cells at the G_0−G_1 phase in pancreatic cancer cells (PANC-1, AsPC-1, BxPC-3 cells) [26]. Additionally, RSV has also been reported to cause S phase arrest in many other cell types [28-30].

In this study, RSV and HU treatment resulted in similar decrease in percentage of cells at G_2/M phase (Fig. 3). RSV at low concentration induced cell cycle arrest at G_0/G_1 phase. Indeed, RSV could block the G_1/S transition of the cell cycle by regulating the protein expression of cyclin D1, D2, and the activities of various kinases as previously reported [31-32]. However, similar to HU, RSV at high concentration induced accumulation of cells at S phase as documented in previous reports [33-35]. RSV showed the function of reducing cell growth and inhibiting cell proliferation through directly acting on cell cycle arrest at S phase in A549 cells.

Cellular RNR expression after RSV and HU treatment

It has been suggested that the perturbation nucleotide metabolism could be caused by the inhibitory effects of RSV on the enzyme RNR. RNR is the key enzyme of de novo DNA synthesis. The enzyme needs a tyrosl free radical for its activity and can therefore be inhibited by free radical scavengers, such as RSV and HU [36-39]. The ability of RSV to destroy the tyrosyl radical was correlated with its strong dose-dependent inhibitory effects on RNR activity [36-37]. In this study, RSV at different concentrations and HU have no effect on protein expression of RRM1, RRM2 and P53R2 in A549 cells after 24 h treatment (Fig. 4). These findings were consistent with previous reports that the inhibition effect of RSV on RNR could derive from reducing RNR activity by scavenging tyrosyl free radicals like HU does rather than decreasing RNR expression [14, 19, 36-39].

Dual effects of high concentration RSV on A549 cells

RSV at high concentration had a significant cytotoxicity effect on A549 cells while exerting no cytotoxicity at low concentration after 24 h treatment. Our results revealed that, in A549 cells, the effect of RSV on nucleotide metabolism varied dramatically depending on the concentration. RSV at 25 μmol·L^{-1} caused no remarkable perturbation of dRNs pools. However, when treatment concentration was increased to 100 μmol·L^{-1}, severe decreases in many dRNs, especially dNTPs were observed, which could subsequently inhibit DNA synthesis. Simultaneously, RSV at 100 μmol·L^{-1} induced enrichment of A549 cells in S phase, in which the cells should

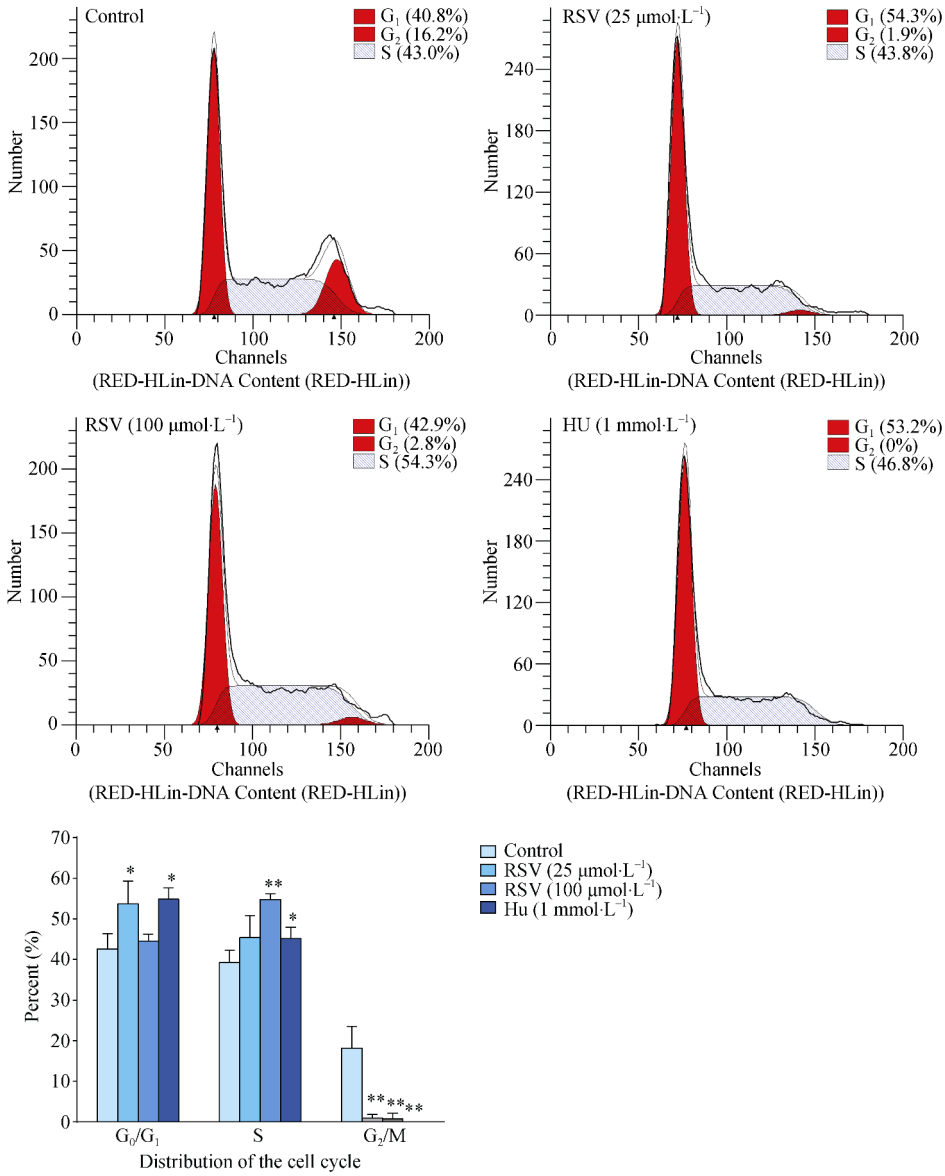

Fig. 3 Cell cycle distribution of A549 cells after RSV and HU treatment. The images of cell cycle distribution are presented as one experiment representative of 3 experiments with similar results. The quantitative data was represented as mean ± SD (n = 3), $^{*}P < 0.05$, $^{**}P < 0.01$ *vs* control group

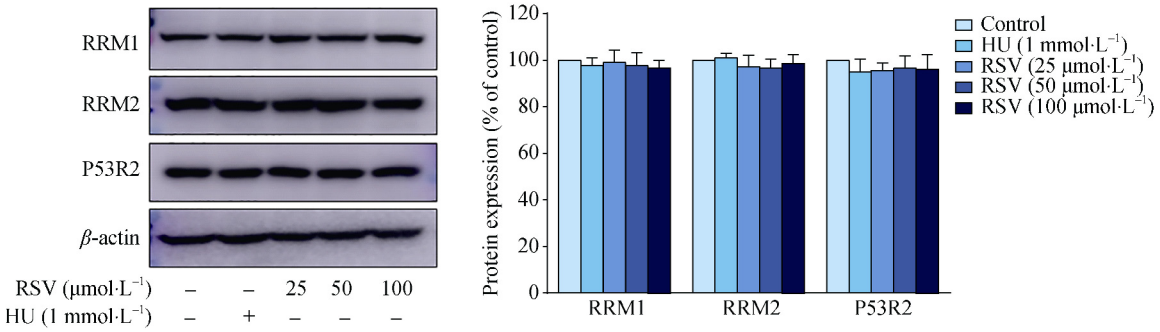

Fig. 4 Western blot analysis of the effect of RSV and HU on expression of RNR subunits M1 (RRM1) and M2 (RRM2), P53-controlled ribonucleotide reductase (P53R2). The images of cell cycle distribution are presented as one experiment representative of 3 experiments with similar results. The quantitative data was represented as mean ± SD (n = 3), $^{*}P < 0.05$, $^{**}P < 0.01$ *vs* control group

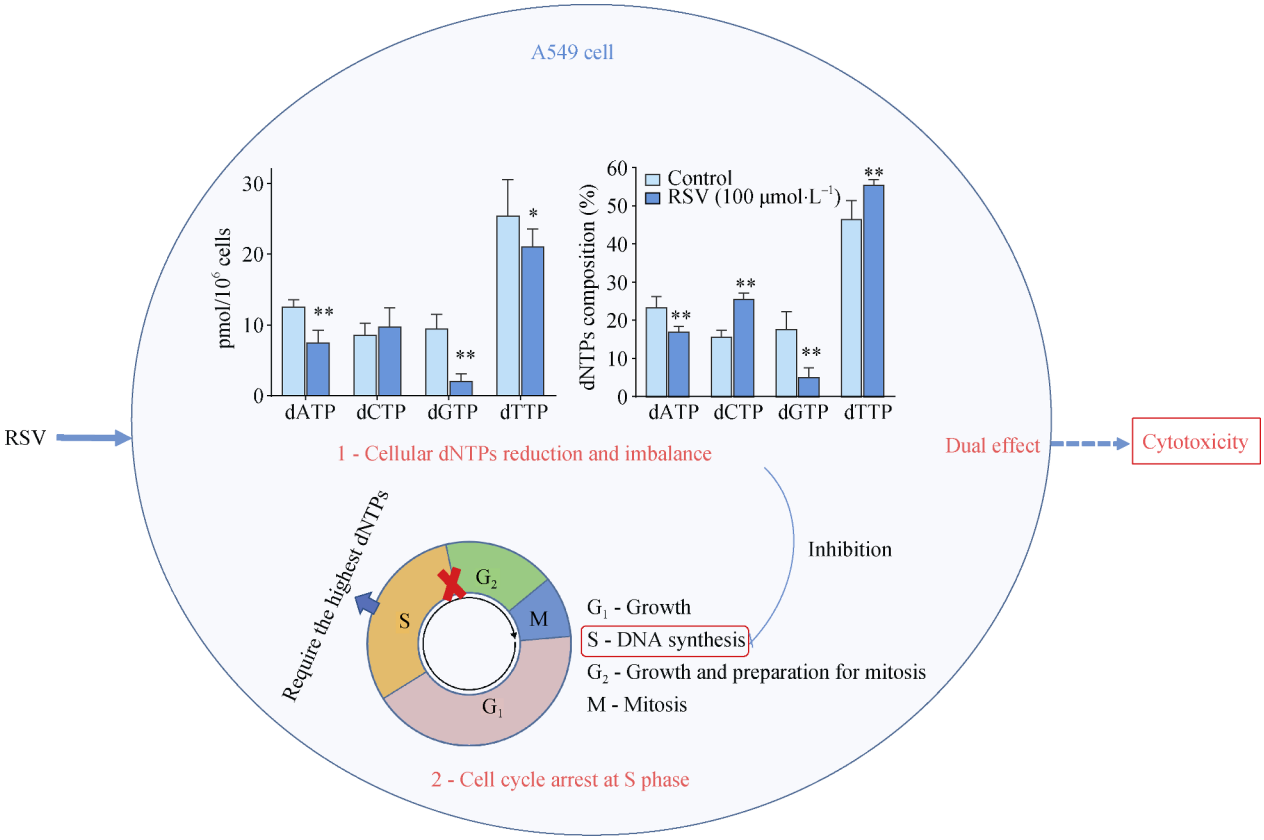

Fig. 5 Putative mechanisms elucidating the cytotoxicity effect of resveratrol on A549 cells. RSV at high dose induces a dual effect including S phase arrest and DNA synthesis inhibition, which may respond for its cytotoxicity effect. The quantitative data was represented as mean ± SD (n = 3), $^{*}P < 0.05$, $^{**}P < 0.01$ *vs* control group

be actively proliferating with highest dNTPs pools than other phases. However, the inhibitory effect of RSV at 100 μmol·L^{-1} on DNA synthesis limited the subsequent progression through S phase in A549 cells. Nevertheless, HU caused similar dNTPs perturbation but slighter S phase arrest as high concentration RSV does, consequently no cytotoxicity effect. Therefore, the dual effect of high concentration RSV including induction of S phase and inhibition of DNA synthesis, may be responsible for its cytotoxicity effect (Fig. 5).

Conclusion

Our findings confirmed that the effects of RSV on perturbation of cellular nucleotide pools and cell cycle distribution were correlated with treated concentrations. RSV at high concentration resulted in significant decreases in dNTPs pools which could inhibit DNA synthesis, while RSV at low concentration had no remarkable effect on dRNs pools. Meanwhile, RSV at high concentration induced cell cycle arrest at S phase, in which the cells required the highest dNTPs supply than other phases for DNA replication. However, the inhibition of DNA synthesis induced by RSV at 100 μmol·L^{-1} limited the subsequent progression through S phase in A549 cells. Therefore, this dual effects of high concentration RSV on two important processes in cell cycle progression, S phase arrest and DNA synthesis inhibition, may be responsible for its cytotoxicity effect. The unique features of RSV provide important clues to the molecular mechanisms of its anticancer effect on epithelial cells, and suggest its potential usefulness as an adjuvant in chemotherapy of lung adenocarcinoma.

References

[1] Baur JA, Sinclair DA. Therapeutic potential of resveratrol: the *in vivo* evidence [J]. *Nat Rev Drug Discov*, 2006, **5**(6): 493-506.

[2] Pirola L, Fröjdö S. Resveratrol: one molecule, many targets [J]. *IUBMB Life*, 2008, **60**(5): 323-332.

[3] Li H, Xia N, Förstermann U. Cardiovascular effects and molecular targets of resveratrol [J]. *Nitric oxide*, 2012, **26**(2): 102-110.

[4] Jang JY, Min JH, Wang SB, *et al*. Resveratrol inhibits collagen-induced platelet stimulation through suppressing NADPH oxidase and oxidative inactivation of SH2 domain-containing protein tyrosine phosphatase-2 [J]. *Free Radical Bio Med*, 2015, **89**: 842-851.

[5] Valdecantos MP, Pérez-Matute P, Quintero P, *et al*. Vitamin C, resveratrol and lipoic acid actions on isolated rat liver mitochondria: all antioxidants but different [J]. *Redox Rep*, 2010, **15**(5): 207-216.

[6] Tung BT, Rodríguez-Bies E, Talero E, *et al*. Anti-inflammatory effect of resveratrol in old mice liver [J]. *Exp Gerontol*, 2015, **64**: 1-7.

[7] Varshney P, Dey CS. Resveratrol regulates neuronal glucose uptake and insulin sensitivity *via* P21-activated kinase 2 (PAK2) [J]. *Biochem Bioph Res Co*, 2017, **485**(2): 372-378.
[8] Sadi G, Bozan D, Yildiz HB. Redox regulation of antioxidant enzymes: post-translational modulation of catalase and glutathione peroxidase activity by resveratrol in diabetic rat liver [J]. *Mol Cell Biochem*, 2014, **393**(1-2): 111-122.
[9] Kuršvietienė L, Stanevičienė I, Mongirdienė A, *et al*. Multiplicity of effects and health benefits of resveratrol [J]. *Medicina*, 2016, **52**(3): 148-155.
[10] Gwak HR, Kim S, Dhanasekaran DN, *et al*. Resveratrol triggers ER stress-mediated apoptosis by disrupting N-linked glycosylation of proteins in ovarian cancer cells [J]. *Cancer Lett*, 2016, 371(2): 347-353.
[11] Selvaraj S, Sun Y, Sukumaran P, *et al*. Resveratrol activates autophagic cell death in prostate cancer cells *via* downregulation of STIM1 and the mTOR pathway [J]. *Mol Carcinogen*, 2016, **55**(5): 818-831.
[12] Alayev A, Salamon RS, Schwartz NS, *et al*. Combination of rapamycin and resveratrol for treatment of bladder cancer [J]. *J Cell Physiol*, 2017, **232**(2): 436-446.
[13] Rauf A, Imran M, Butt MS, *et al*. Resveratrol as an anti-cancer agent: A review [J]. *Crit Rev Food Sci*, 2018, **58**(9): 1428-1447.
[14] Fontecave M, Lepoivre M, Elleingand E, *et al*. Resveratrol, a remarkable inhibitor of ribonucleotide reductase [J]. *FEBS Lett*, 1998, **421**(3): 277-279.
[15] Subbaramaiah K, Chung WJ, Michaluart P, *et al*. Resveratrol inhibits cyclooxygenase-2 transcription and activity in phorbol ester-treated human mammary epithelial cells [J]. *J Biol Chem*, 1998, **273**(34): 21875-21882.
[16] Szekeres T, Saiko P, Fritzer‐Szekeres M, *et al*. Chemopreventive effects of resveratrol and resveratrol derivatives [J]. *Ann NY Acad Sci*, 2011, **1215**(1): 89-95.
[17] Crona M, Codó P, Jonna VR, *et al*. A ribonucleotide reductase inhibitor with deoxyribonucleoside-reversible cytotoxicity [J]. *Mol Oncol*, 2016, **10**(9): 1375-1386.
[18] Mah V, Alavi M, Márquez-Garbán DC, *et al*. Ribonucleotide reductase subunit M_2 predicts survival in subgroups of patients with non-small cell lung carcinoma: effects of gender and smoking status [J]. *PLoS One*, 2015, **10**(5): e0127600.
[19] Elford HL, Freese M, Passamani E, *et al*. Ribonucleotide reductase and cell proliferation. I. Variations of ribonucleotide reductase activity with tumor growth rate in a series of rat hepatomas [J]. *J Biol Chem*, 1970, **245**(20): 5228-5233.
[20] Zhang W, Tan S, Paintsil E, *et al*. Analysis of deoxyribonucleotide pools in human cancer cell lines using a liquid chromatography coupled with tandem mass spectrometry technique [J]. *Biochem Pharmacol*, 2011, **82**(4): 411-417.
[21] Zegerman P, Diffley JF. DNA replication as a target of the DNA damage checkpoint [J]. *DNA Repair*, 2009, **8**(9): 1077-1088.
[22] Pai CC, Kearsey S. A critical balance: dNTPs and the maintenance of genome stability [J]. *Genes*, 2017, **8**(2): 57.
[23] Varoni EM, Lo Faro AF, Sharifi-Rad J, *et al*. Anticancer molecular mechanisms of resveratrol [J]. *Front Nutr*, 2016, **3**: 8.
[24] Yuan L, Zhang Y, Xia J, *et al*. Resveratrol induces cell cycle arrest *via* a p53-independent pathway in A549 cells [J]. *Mol Med Rep*, 2015, **11**(4): 2459-2464.
[25] Bai Y, Mao QQ, Qin J, *et al*. Resveratrol induces apoptosis and cell cycle arrest of human T24 bladder cancer cells *in vitro* and inhibits tumor growth *in vivo* [J]. *Cancer Sci*, 2010, **101**(2): 488-493.
[26] Cui J, Sun R, Yu Y, *et al*. Antiproliferative effect of resveratrol in pancreatic cancer cells [J]. *Phytother Res*, 2010, **24**(11): 1637-1644.
[27] Delmas D, Lançon A, Colin D, *et al*. Resveratrol as a chemopreventive agent: a promising molecule for fighting cancer [J]. *Curr Drug Targets*, 2006, **7**(4): 423-442.
[28] Fulda S, Debatin KM. Sensitization for tumor necrosis factor-related apoptosis-inducing ligand-induced apoptosis by the chemopreventive agent resveratrol [J]. *Cancer Res*, 2004, **64**(1): 337-346.
[29] Castello L, Tessitore L. Resveratrol inhibits cell cycle progression in U937 cells [J]. *Oncol Rep*, 2005, **13**(1): 133-138.
[30] Yu XM, Jaskula-Sztul R, Ahmed K, *et al*. Resveratrol induces differentiation markers expression in anaplastic thyroid carcinoma *via* activation of Notch1 signaling and suppresses cell growth [J]. *Mol Cancer Ther*, 2013, **12**(7): 1276-1287.
[31] Whyte L, Huang YY, Torres K, *et al*. Molecular mechanisms of resveratrol action in lung cancer cells using dual protein and microarray analyses [J]. *Cancer Res*, 2007, **67**(24): 12007-12017.
[32] Gu S, Chen C, Jiang X, *et al*. ROS-mediated endoplasmic reticulum stress and mitochondrial dysfunction underlie apoptosis induced by resveratrol and arsenic trioxide in A549 cells [J]. *Chem-Biol Interact*, 2016, **245**: 100-109.
[33] Kim Y, Lee WH, Choi TH, *et al*. Involvement of p21WAF1/CIP1, pRB, Bax and NF-κB in induction of growth arrest and apoptosis by resveratrol in human lung carcinoma A549 cells [J]. *Int J Oncol*, 2003, **23**(4): 1143-1149.
[34] Liao HF, Kuo CD, Yang YC, *et al*. Resveratrol enhances radiosensitivity of human non-small cell lung cancer NCI-H838 cells accompanied by inhibition of nuclear factor-kappa B activation [J]. *J Radiat Res*, 2005, **46**(4): 387-393.
[35] Kaminski MB, Steinhilber DM Stein J, *et al*. Phytochemicals resveratrol and sulforaphane as potential agents for enhancing the anti-tumor activities of conventional cancer therapies [J]. *Curr Pharm Biotechno*, 2012, **13**(1): 137-146.
[36] Fontecave M, Lepoivre M, Elleingand E, *et al*. Resveratrol, a remarkable inhibitor of ribonucleotide reductase [J]. *FEBS Lett*, 1998, **421**(3): 277-279.
[37] Szekeres T, Fritzer-Szekeres M, Saiko P, *et al*. Resveratrol and resveratrol analogues-structure-activity relationship [J]. *Pharm Res*, 2010, **27**(6): 1042-1048.
[38] Saban N, Bujak M. Hydroxyurea and hydroxamic acid derivatives as antitumor drugs [J]. *Cancer Chemoth Pharm*, 2009, **64**(2): 213.
[39] Osterman Golkar S, Czene S, Gokarakonda A, *et al*. Intracellular deoxyribonucleotide pool imbalance and DNA damage in cells treated with hydroxyurea, an inhibitor of ribonucleotide reductase [J]. *Mutagenesis*, 2013, **28**(6): 653-660.

Cite this article as: LI Zheng, CHEN Qian-Qian, LAM Christopher Wai Kei, GUO Jian-Ru, ZHANG Wei-Jia, WANG Cai-Yun, WONG Vincent Kam Wai, YAO Mei-Cun, ZHANG Wei. Investigation into perturbed nucleoside metabolism and cell cycle for elucidating the cytotoxicity effect of resveratrol on human lung adenocarcinoma epithelial cells [J]. *Chin J Nat Med*, 2019, **17**(8): 608-615.